Wolf-Rayet Phenomena in Massive Stars and Starburst Galaxies
Proceedings IAU Symposium No. 193, ©1999 IAU
K.A. van der Hucht, G. Koenigsberger & P.R.J. Eenens, eds.

H II galaxies as distance estimators at high redshift

Jorge Melnick[1], Roberto J. Terlevich[2,3], Elena Terlevich[3], and Benoit Joguet[1]

[1]*European Southern Observatory, Casilla 19001, Santiago 19, Chile*
[2]*Institute of Astronomy, Madingley Road, Cambridge CB3 0EZ, UK*
[3]*INAOE, Apartado Postal 51, 72000, Puebla, Mexico*

Abstract. Owing to their large luminosities per unit mass H II galaxies allow us to investigate in considerable detail the process of high mass star formation out to redshifts of cosmological importance. In this contribution we discuss the calibration of the correlation between the Hβ luminosity and the emission line width of H II galaxies as a distance indicator. We show that H II galaxies can be reliably used as distance indicators out to redshifts $z > 3$ provided that their line widths and fluxes can be determined with accuracies better than 10%.

1. Introduction

H II galaxies are dwarf galaxies whose (bolometric) luminosity is dominated by very young stellar populations. Because of their large luminosity per unit mass, in spite of their low masses H II galaxies can be observed out to distances of cosmological interest. This opens a gate through which we can glance at the processes of massive star formation when the Universe had a small fraction of its present age. We are not there yet as the new generation of IR spectrometers on 8m class telescopes are required to cross that gate, but it is timely to examine what we have learned from our local neighborhood in order to prepare the jump to deep cosmological space.

In this contribution[1] we would like to revisit the use of H II galaxies as distance estimators by reviewing the status of the correlation between integrated emission line luminosities, L, and the width of their emission line profiles, σ.

2. The L(Hβ)–σ relation for H II galaxies

Terlevich & Melnick (1981; henceforth TM) showed that there is a very strong correlation between line-width and Hβ luminosity for H II galaxies. Based on the similarity between this correlation and the L–σ relation for ellipticals and spiral bulges, they argued that the widths of the emission lines in H II galaxies could be used to measure their total masses. The correlation was calibrated as a distance indicator by Melnick *et al.* (1988; henceforth MTM) who showed that, in fact, the correlation was a fundamental plane with oxygen abundance

[1]Based on research done at the III Guillermo Haro Workshop

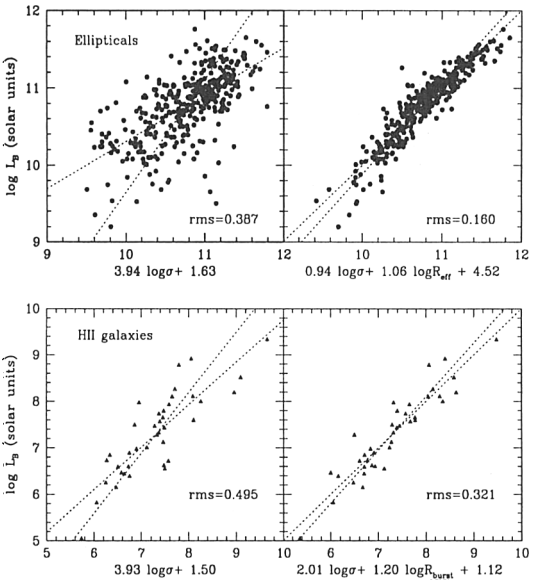

Figure 1. Comparison between the L–σ relations and fundamental planes for ellipticals and H II galaxies from Telles (1995).

(O/H) as the third dimension. Recently Telles (1995) measured radii for a subsample of the MTM galaxies and showed that the fundamental plane resembles very closely the D_n–σ relation for Ellipticals. Figure 1 shows Telles' comparison between ellipticals and H II galaxies.

These observations lend strong support to the conclusion reached by Terlevich and Melnick that the ionized gas in H II galaxies[2] is in Virial equilibrium with the total mass of the young component.

Figure 2 shows the $L(\mathrm{H}\beta)$–σ relation plotted using the data of MTM for local objects plus galaxies at intermediate and high redshifts from the literature (Koo *et al.* 1995; Guzman *et al.* 1997; Pettini *et al.* 1998). The solid line shows the MTM-fit to the local objects. Because no extinction measurements are available for the intermediate ($z > 0.1$) and high ($z \sim 3$) redshift galaxies, the MTM galaxies are plotted in Figure 2 without extinction corrections.

Figure 2 shows that the correlation is satisfied by objects out to very large redshifts, and that the most distant objects have luminosities similar to those of the most luminous galaxies in the local sample. This reassures us that the high-z galaxies are indeed H II galaxies.

There are a number of systematic effects in the correlation that must be understood before it can be used as an unbiased distance indicator. These are discussed below.

[2]There is still little information about the old stellar populations in many of these objects

https://doi.org/10.1017/S0074180900206591 Published online by Cambridge University Press

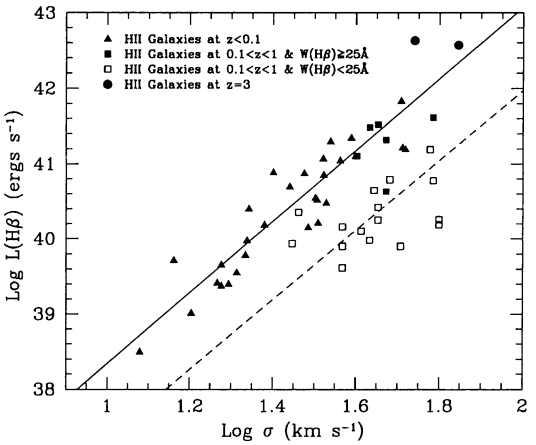

Figure 2. The L–σ correlation for H II galaxies at a wide range of redshifts. The solid line shows the Maximum-Likelihood fit to the young H II galaxies in the local Universe. The dashed line shows the predicted $L(\mathrm{H}\beta)$–σ relation for an evolved population of H II galaxies.

2.1. Kinematic effects

MTM have shown that objects with $\sigma > 65\,\mathrm{km\,s^{-1}}$ are probably affected by rotation of the parent galaxies or kinematic influence from underlying old stellar populations. The same result was found by Koo *et al.* (1995) for intermediate redshift objects. This cutoff can be understood if one assumes that the gas in H II galaxies is in Virial equilibrium with the rest of the galaxy (Terlevich and Melnick, 1981; MTM). Using the Virial theorem the limit of $65\,\mathrm{km\,s^{-1}}$ results from equating the free-fall time to the main-sequence life time of the most massive stars, which should be the same if H II galaxies are powered by coeval starburst clusters. One of the high-z objects plotted in Figure 1 appears to exceed this limit but the measurement uncertainty ($\pm 20\,\mathrm{km\,s^{-1}}$), is still rather large.

Although the case for gravity as the source of line broadening in H II galaxies is strong, recent studies of the gas dynamics in giant H II regions suggest that the case cannot be closed yet. Giant extragalactic H II regions exhibit the same L–σ relation as H II galaxies and this allowed MTM to use them to fix the zero-point of the correlation. The detailed gas kinematics of two prototypical giant H II regions, 30 Dor and NGC 604, have recently been shown to be very different (Melnick *et al.* 1999 and references therein).

The spatially integrated line-profile width of 30 Doradus is dominated by stellar-wind driven expanding shells and filaments, while that of NGC 604 is probably dominated by gravity or other as yet not understood mechanism; the profiles at most positions within NGC 604 are well fitted by single Gaussians of widths comparable to that of the integrated light. In 30 Doradus, on the other hand, the profiles at most positions have multiple components of widths much smaller than its integrated line-width. Moreover, the radial velocity dispersion of

https://doi.org/10.1017/S0074180900206591 Published online by Cambridge University Press

NGC 604 is much smaller than its line width, while in 30 Dor the radial velocity dispersion and integrated line-profile width are comparable.

In view of these differences, it is surprising that both nebulae fit so well the L–σ relation (Melnick *et al.* 1987). If the Hβ luminosities of H II galaxies are due to one or more giant H II region components, we would in principle expect them to show similar differences in their global gas kinematics although the results of Telles (1995) indicate that at the scales of H II galaxies, differences in the detailed gas hydrodynamics may be small compared to the effect of gravity.

2.2. Age effects

In order to minimize systematic effects due to the rapid evolution of the ionizing stars, MTM restricted their sample to galaxies with $W(\mathrm{H}\beta) > 25$Å. In fact, this restriction has a double purpose which is particularly relevant for high-z objects: it selects only young starbursts, and it eliminates objects with significant underlying old(er) stellar populations. The latter is critical because an old stellar population may widen the emission lines is a way that is uncorrelated with the total mass of the young component and hence with its emission line luminosity.

There are only a few objects in our intermediate redshift sample with $W(\mathrm{H}\beta) > 25$Å. These are plotted with filled symbols in Figure 2. The open symbols show the data for objects with weaker lines. As expected, these objects do not fit the correlation defined by the local H II galaxies which have a mean line strength of $< W(\mathrm{H}\beta) > = 105$Å. The discrepancy is mostly due to luminosity evolution because the Hβ luminosities of the Koo *et al.* (1995) and Guzmán *et al.* (1997) galaxies are derived from the blue magnitudes and equivalent widths.

The luminosity evolution of a young coeval starburst during the first 10^7yr proceeds as a rapid decay of the emission line flux after the first 3 Myr at roughly constant continuum flux until about 6 Myr so in that range of ages the age-dimming in $L(\mathrm{H}\beta)$ can be directly estimated from the change in equivalent widths (Terlevich & Melnick, 1981; Copetti, Pastoriza & Dottori, 1986). The mean equivalent width of the objects plotted as open squares in Figure 2 is $< W(\mathrm{H}\beta) > = 11$Å so evolution reduces the average Hβ luminosity of the sample by a factor 105/11. The dashed line shows the MTM relation affected by this amount of evolution. The fit is seen to be more than acceptable, confirming our conclusion that most objects are evolved starbursts rather than strong starbursts on top of a bright, older stellar population. Note, however, that two of the weak-lined galaxies fit the correlation without luminosity corrections. These objects have very strong lines, but also very strong continua, indicating the presence of a significant underlying older stellar population. The HST images of one of these galaxies (H1-3618) by Koo *et al.* (1994) show that this object is very compact indicating that the strong continuum is most likely the light from an older starburst.

Another indication that the objects in the intermediate redshift sample are in general more evolved than the local sample comes from the excitation of the nebular gas as measured by the ratio of [OIII]/Hβ. The mean value from Guzmán *et al.* (1997) is $<$[OIII]/H$\beta$$> = 2.2 \pm 0.5$ while the mean for the MTM sample is $<$[OIII]/H$\beta$$> = 5 \pm 2$.

https://doi.org/10.1017/S0074180900206591 Published online by Cambridge University Press

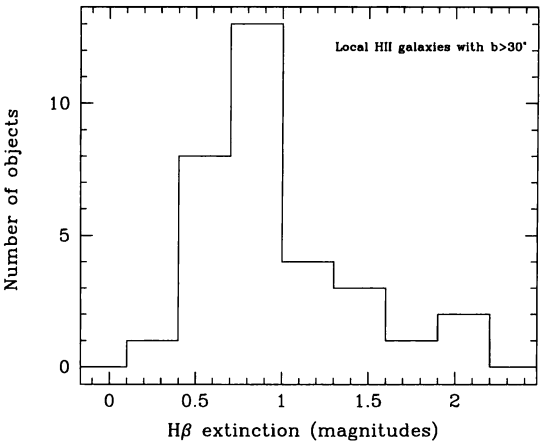

Figure 3. Distribution of extinction measured from the Balmer decrements for local H II galaxies at high galactic latitudes ($b > 30°$).

2.3. Extinction effects

Extinction corrections for local H II galaxies are determined in a straightforward manner from the Balmer decrements (MTM). Figure 3 presents a histogram of the extinction for the MTM galaxies at high galactic latitudes ($b > 30°$) in order to minimize the contribution of foreground galactic extinction. The extinction is strongly peaked at a value of $A_{H\beta} = 0.8$ mag, with a median of about $A_{H\beta} = 1$ mag which is also typical of giant extragalactic H II regions. (Melnick *et al.* 1987).

It is rather difficult to measure the Balmer decrements from low S/N observations of intermediate and high redshift H II galaxies and it is normally not done. Therefore, all the luminosities plotted in Figure 2 are without extinction corrections.

2.4. Metallicity effects

MTM have shown that the $L(H\beta) - \sigma$ relation is in fact a 'fundamental plane' where the third dimension can be parametrized by the oxygen abundance (O/H). Recently, Telles (1995) has shown that the effective radius of the ionizing clusters can also be used as a third parameter, and that the fundamental plane thus defined by H II galaxies is remarkably similar to that exhibited by ellipticals. In the calibration of the ($L(H\beta) - \sigma$) as a distance indicator, MTM found an important systematic shift in luminosity between the giant H II regions in nearby late type galaxies used to determine the zero point, and the H II galaxies which is due to differences in the mean metallicities of the two samples.

The distribution of metallicities for the 34 MTM H II galaxies in the local sample is presented in Figure 4. Unfortunately, there are no metallicities available yet for the intermediate and high redshift objects, but clearly, in order to use the $L(H\beta) - \sigma$ relation as a distance indicator, either the metallicities of the

https://doi.org/10.1017/S0074180900206591 Published online by Cambridge University Press

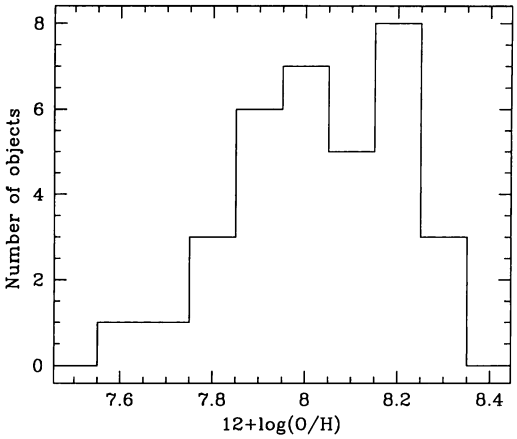

Figure 4. Distribution of Oxygen abundances for H II galaxies in the local Universe ($z < 0.1$).

local and high-z samples must be similar, or the luminosities must be corrected using O/H as prescribed by MTM.

In a pilot project to measure accurate metallicities and electron temperatures of H II galaxies at redshifts between 0.2 and 1 (Terlevich *et al.* in preparation) we observed a sample of 20 low metallicity candidates with the *ESO* 3.6m and *NTT* telescopes. We could clearly detect the faint electron temperature sensitive line [OIII]λ4363Å in the spectra of the five objects with largest $W(\mathrm{H}\beta)$. A preliminary analysis of the data yields a mean oxygen abundance of $<12+\log(\mathrm{O/H})> = 7.8$ lower, in fact, than the mean value for the local sample. This provides very tentative evidence that higher redshift objects could be systematically poorer in metals, although the data are still very sparse and inaccurate, to allow this indication to be more than just a hint.

3. Multiplicity

As we have seen in this meeting and also in the work of Telles *et al.* (1997) a significant fraction of H II galaxies have multiple young components. Thus, depending on how the observations are done, this could introduce a systematic bias in the L–σ relation since the mass that binds these components together is in principle not related to the Hβ luminosity but may influence σ. This is a tricky effect because it depends not only on the mass of old stellar population, but also on its detailed kinematics, inclination, etc. A preliminary study using the Telles *et al.* 1997 sample did not reveal any systematic effects of multiplicity in the $L(\mathrm{H}\beta)$–σ relation (Joguet & Melnick 1999).

https://doi.org/10.1017/S0074180900206591 Published online by Cambridge University Press

4. H II galaxies as cosmological probes

There is evidence from a number of independent venues that the value of the cosmological constant (Λ) may be different from zero (see *e.g.*, Lineweaver, 1998 for a recent review). A very interesting feature of the Hubble diagrammes with cosmological constant is the so-called *focusing effect* mentioned by Refsdal *et al.* (1967). This is shown in Figure 5 that plots the predicted luminosity distance (normalized to $\Omega_M = 0.5$ and $\Omega_\Lambda = 0$) as a function of redshift for different combinations of cosmological parameters and for $H_o = 65\,km\,s^{-1}\,Mpc^{-1}$. For a given Ω_M the world models of different Ω_Λ converge and the convergence increases with mass density. For $\Omega_M = 0$ (not shown in the figure) there is no convergence while for $\Omega_M > 1$ the models for all values of Ω_Λ converge on a point close to $z = 2$.

This effect allows the accurate determination of Ω_M independently of Ω_Λ. For small Ω_M the optimum redshift range is $z \simeq 3$ where already a large sample of H II galaxies does exist. The existence of this focusing also implies that the best range to determine Ω_Λ using the magnitude-redshift method is either $z < 1$ or $z > 5$.

H II galaxies provide possibly the only technique that allows to determine distances to objects from the local group to $z > 3$. Ellipticals and spirals are bedeviled by evolutionary effects in their stellar populations (Vogt *et al.* 1997; Rix *et al.* 1997) while SN Ia, potentially the most accurate technique, is presently limited to $z < 1$ (*e.g.*, Perlmutter *et al.* 1999; Riess *et al.* 1998 and references therein). In order to illustrate the application of H II galaxies to cosmology, we have calculated the predicted distances for the objects plotted in Figure 2 using the most recent data for the distance moduli and abundances for local giant H II

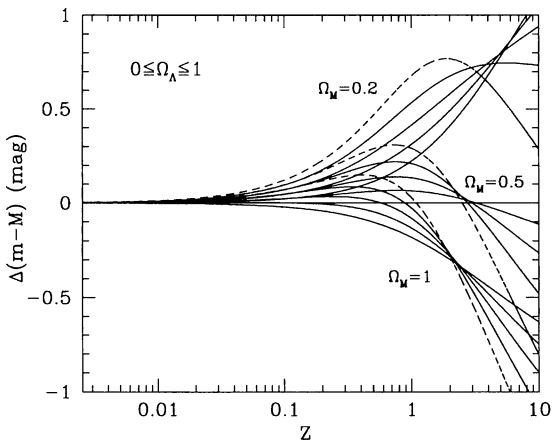

Figure 5. Normalized DM $\Delta(m-M) = (m-M)_{\Omega_M,\Omega_\Lambda} - (m-M)_{.5,0}$ as a function of redshift. For each value of Ω_M as labeled in the Figure we plot a family of vacuum density $\Omega_\Lambda = 0, 0.25, 0.5, 0.75, 1.0$. For each family, the dashed line corresponds to $\Omega_\Lambda = 0$. All models are for $H_o = 65$.

https://doi.org/10.1017/S0074180900206591 Published online by Cambridge University Press

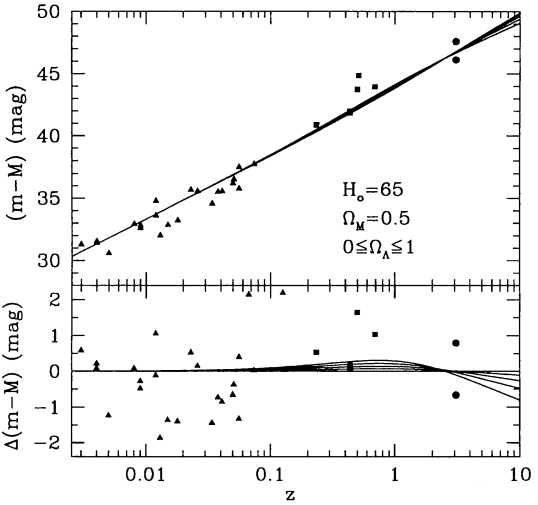

Figure 6. *Top panel:* The Hubble diagram for H II galaxies of a wide range of redshifts. The family of curves for $\Omega_M = 0.5$ from Figure 5 is shown. *Bottom panel:* the same diagram normalized to $\Omega_\Lambda = 0$ to enhance the separation between different models.

regions available in the literature to re-calibrate the zero point of the unbiased distance indicator introduced by MTM, $M_Z = \frac{\sigma^5}{O/H}$. The new calibration is thus given by,

$$log\, L(\mathrm{H}\beta) = log M_Z + 29.5$$

from which the distance modulus is obtained as,

$$log(m - M) = 2.5 \times log\frac{\sigma^5}{\mathrm{F}(\mathrm{H}\beta)} - 2.5 \times log(O/H) - A_\beta - 26.44 \qquad 1$$

where $\mathrm{F}(\mathrm{H}\beta)$ is the observed $\mathrm{H}\beta$ flux and $A_{\mathrm{H}\beta}$ is the total extinction.

Figure 6 presents the resulting Hubble diagramme for H II galaxies. The lines show the $\Omega_M = 0.5$ family of models from Figure 5. We have used constant values of $A_{\mathrm{H}\beta} = 1$ and $\log(\mathrm{O/H}) = -4.2$ for all galaxies at $z > 0.1$ to compute their distance moduli. These values correspond to the median extinction of the local sample and to the mean abundance of our pilot project galaxies discussed in Section 5.3

Although this data set cannot at this stage be used to limit the cosmological parameters, it gives an indication of the quality and quantity of data needed to set meaningful limits to these parameters, and of the effects of random and systematic errors. Extinction and metallicity have the same sign in Eq.1. Systematic changes of 0.2 dex in O/H and 0.2 mag in extinction translate into shifts of 0.7 mag in distance modulus. It is entirely possible, therefore, that the discrepancy in $(m - M)$ for the $z = 3$ galaxies be due to differences in these parameters, although the observational errors are very large. Since the maximum separation

https://doi.org/10.1017/S0074180900206591 Published online by Cambridge University Press

between $\Omega_M = 0.2$ and $\Omega_M = 1$ at $z = 3$ is about one magnitude, it is crucial to have control over the systematics in order to use H II galaxies to constrain Ω_M. Clearly, for low redshift objects the scatter is totally dominated by observational errors and in particular by errors in the line widths which range between 5% and 15% (MTM). We believe that using the new optical and IR spectrographs that are coming on-line on 8m-class telescopes it will be possible to measure F(Hβ) to better than 20% and σ to better than 10% at $z = 3$. An accurate determination of Ω_M, therefore, will be possible with samples of a few tens of objects. The determination of extinction and metallicity at this redshift will be challenging due to contamination by strong atmospheric lines.

5. Conclusions

Our exploration of the use of the redshift-magnitude method to determine the cosmological constant (Ω_Λ) and the mass density of the Universe (Ω_M) using H II galaxies led us to re-discover the important focusing effect in Λ for redshifts about 3. This effect implies that the apparent magnitude at redshifts close to 2–3 has almost no dependence on Ω_Λ for $\Omega_M > 0.2$.

Our strong conclusion is that using the redshift-magnitude diagram method Ω_M can be measured independently of the value of Ω_Λ by targeting the redshift range according to an estimate of the value of Ω_M. In particular, for small Ω_M, the optimum redshift is $z \simeq 3$.

We also find that the best range to determine Ω_Λ using the redshift-magnitude method is well away from the redshift region where the focusing occurs, *i.e.*, either $z < 1$ or $z > 5$.

Considering that we have very little control over the systematic effects discussed above for galaxies at $z > 0.1$, we find it quite remarkable that the $L(\mathrm{H}\beta) - \sigma$ relation established by MTM for local H II galaxies is so well satisfied by objects of a wide range of redshifts extending up to $z \simeq 3$. Furthermore, the intermediate redshift sample itself shows a $L(\mathrm{H}\beta) - \sigma$ correlation similar to that found in the local universe.

An important aspect to bear in mind is that none of the intermediate and high redshift H II galaxies found thus far has very strong emission lines. For most objects this may be an effect of evolution plus the fact that we have not yet found the youngest galaxies at high redshifts. This is not surprising because all the intermediate and high redshift objects we have used in this paper have been discovered using broad-band photometric techniques that miss objects with very weak continua. Searches are underway using narrow band techniques that are revealing objects with redshifts $z > 3$ and strong Lyman-α lines (Hu *et al.* 1998). We think that many of these objects may in fact be young H II galaxies. Using the high efficiency IR spectrographs that are becoming available in the new generation of 8–10m telescopes it will be possible to determine the Hβ line widths, luminosities, and equivalent widths of these objects with high accuracy. This will allow for the first time to probe the cosmological parameters out to unprecedented distances using the distance estimator.

https://doi.org/10.1017/S0074180900206591 Published online by Cambridge University Press

References

Copetti, M.V.F., Pastoriza, M.G. Dottori, H.A. 1986, A&A 156, 243
Goobar, A., Perlmutter, S. 1995, ApJ 450, 14
Guzmán, R., Gallego, J., Koo, D.C. *et al.* 1997, ApJ 489, 559
Koo, D.C., Guzmán, R., Faber, S.M. *et al.* 1995, ApJ 440, L49
Koo, D.C., Vogt, N.P., Phillips, A.C. *et al.* 1996, ApJ 469, 535
Hu, E., Cowie, L.L., McMahon, R.G., 1998, ApJ 502, L99
Joguet, B., Melnick, J. 1999, Moriond Workshop in press
Lineweaver, C.H. 1998, ApJ 505, L69
Melnick, J., Moles, M., Terlevich, R. Garcia-Pelayo, J.M. 1987, MNRAS 226, 849
Melnick, J., Terlevich, R., Moles, M. 1988, MNRAS 235, 313 (MTM)
Melnick, J., Tenorio-Tagle, G., Terlevich, R. 1999, MNRAS 302, 677
Perlmutter, S., *et al.* 1999, ApJ in press (astro-ph/9812133)
Pettini, M., Kellogg, M., Steidel, C.C., Dickinson, M., Adelberger, K.L., Giavalisco, M. 1998, ApJ 508, 539
Refsdal, S., Stabell, R. de Lange, F.G. 1967, Memoirs RAS 71, 143
Riess, A.G., Filippenko, A.V., Challis, P. *et al.* 1998, AJ 116, 1009
Rix, H.-W., Guhathakurta, P., Colless, M., Ing, K. 1997, MNRAS 285, 779
Schade, D., Barrientos, L.F., López-Cruz, O. 1997, ApJ 477, L17
Telles, E., 1995, Ph.D. Thesis, Cambridge University
Terlevich, R., Melnick, J. 1981, MNRAS 195, 839
Vogt, N.P., Phillips, A.C., Faber, S.M. *et al.* 1997, ApJ 479, 121

Discussion

Walborn: It's essential to take into account the resolved microstructure in stellar content, nebular geometry, extinction, and kinematics of 30 Dor and N 11, in order to interpret the many distant objects correctly. If one integrates over these structures in the nearby paradigms, there is no hope of disentangling them further away. Walborn & Blades (1997) distinguished five spatially and/or temporally resolved components, of the 30 Dor stellar content, corresponding to discrete epochs of star formation. The nebular emission of 30 Dor is dominated by the curved filaments centered on R 136, which are the interfaces with surrouding molecular clouds where new, triggered star formation is taking place. There are objects with A_V of 20–30 mag in and near these filaments while the extinction toward R 136 is 1.2 mag. Chu has shown that the nebular kinematics of 30 Dor are dominated by multiple discrete shells, due to localized SN and stellar winds, in agreement with the X-ray structure discussed by Wang. N 11 is a giant-shell H II region, which is an evolutionary descendent of the current 30 Dor structure; the morphology of NGC 604 is identical to that of N 11. The *HST*-WFPC2 image of the NCG 4214 starburst shown here by Mas-Hesse and Maíz-Apellániz resolves it into a collection of 30 Dor and N 11 counterparts; your more distant composite object is likely similar.

Melnick: (1) The age spread we find is within one of the Walborn-Blades zones. The two outer OB associations are out of our field and R 136 is not included because of resolution. (2) NGC 604 is fundamentally different from 30 Dor. Here the light is dominated by regions where the profiles are well fitted by single gaussians of intermediate widths. So the integrated line-profile is *not* dominated, and in fact not even affected by expanding shells. The puzzling thing is that the *integrated* profiles of 30 Dor and NGC 604 are

equally well fitted by single gaussians and that these nebulae satisfy the luminosity-line width relation for giant H II regions.

Rosado: A comment. Fabry-Perot data could give quite good results regarding the radial-velocity profile-widths, but is it necessary to have good spatial and spectral resolution in order to separate possible velocity components, otherwise you will see a broad one. An example is the poster by Rosado *et al.* (these Proceedings) on the Hickson H 31 galaxy group, where you see three knots in component B with narrow widths while the integrated spectrum is broad.

Melnick: The F-P spectra of NGC 604 show that most of the pixels accross the face of the nebula have supersonic line-widths. This is most likely not the effect of dilution, because the radial-velocity dispersion of these pixels is sub-sonic everywhere in the nebula.

Homeier: How do you separate rotational broadening from intrinsic line-width of the emitting gas?

Melnick: We use the semi-empirical criterion that $\sigma < 80\,\mathrm{km\,s^{-1}}$.

https://doi.org/10.1017/S0074180900206591 Published online by Cambridge University Press